Effects of Paeoniflorin on the activity of muscle strips, intracellular calcium ion concentration and L-type voltage-sensitive calcium ion channels in the sphincter of Oddi of hypercholesterolemic rabbits

FANG WANG[1], YING YANG[1], XUHUI JI[2], XIONG TAO[2], YUHANG WANG[2] and CHANGMIAO WANG[2]

Departments of [1]Physical Examination and [2]General Surgery, The First Affiliated Hospital of Dalian Medical University, Dalian, Liaoning 116000, P.R. China

Received October 17, 2017; Accepted May 22, 2018

DOI: 10.3892/mmr.2019.10183

Abstract. Sphincter of Oddi dysfunction (SOD) is a benign obstructive disorder predominantly resulting from spasms of the SO. Pharmacological therapies aim to induce SO relaxation; the hypercholesterolemic (HC) rabbit is the only SOD model available for study. In the present study, SO muscle strips, intracellular calcium ion concentrations and the mRNA expression levels of the α1C subunit of the L-type calcium channel in the SO muscle cells of HC rabbits were employed to investigate the effects of paeoniflorin (PF). Alterations in L-type calcium channel α subunit 1C mRNA and protein expression in SO cells with HC following the application of different concentrations of PF were determined by reverse transcription-quantitative polymerase chain reaction and western blotting. The whole cell patch clamp technique was used to observe the effects of different concentrations of paeoniflorin on L-type calcium channel current. The results of the present study demonstrated that PF induced the relaxation of SO muscle strips and reduced the intracellular calcium concentration in the SO muscle cells of HC rabbits. In addition, PF decreased the mRNA expression levels of the α1C subunit of the L-type calcium channel and reduced the L-type calcium channel current in SO cells. These results suggested that the mechanism underlying the relaxation of the SO muscle by PF may be associated with the reduction of calcium ion influx via L-type calcium channels.

Correspondence to: Professor Changmiao Wang, Department of General Surgery, The First Affiliated Hospital of Dalian Medical University, 222 Zhongshan Road, Dalian, Liaoning 116000, P.R. China
E-mail: changmiaowangdoc@163.com

Key words: paeoniflorin, hypercholesterolemia rabbits, sphincter of Oddi, intracellular calcium ion concentration, Ca^{2+} channel

Introduction

Sphincter of Oddi dysfunction (SOD), a benign acalculous obstructive disorder, is characterized by a loss of normal muscular relaxation and contraction, and spasms of the SO (1). SO spasms induce an increase in pressure that obstructs the flow of bile and pancreatic fluid into the duodenum, resulting in a variety of clinical symptoms, including epigastric pain, postprandial bloating, dilation of the common bile duct and the pancreatic duct, increased amylase levels and abnormal hepatic function (2). After almost 20 years of study, it has been reported that SOD not only serves a key role in the pathogenesis of the majority of benign diseases associated with the bile duct and the pancreas, but is also crucial for the secondary pathophysiological changes of these diseases (3). Previously, the management of SOD involved the administration of pharmaceuticals, endoscopic sphincterotomy (ES) and surgical treatment; however, surgical treatment has been superseded by ES. Despite its high success rate (86-91%), the morbidity and mortality associated with ES have been reported to reach 9.8 and 2.3%, respectively (3). The pathogenesis of SOD has not been well documented, and the use of this endoscopic strategy remains highly controversial, as procedural pancreatitis cannot be completely avoided, and surgical treatment may be necessary in certain cases (4). Therefore, pharmacological approaches for the treatment of SOD have been undertaken, such as inducing the relaxation of the SO (5). Antispasmodics, proton pump inhibitors and tricyclic antidepressants have been used to treat SOD in the clinic, but with very limited success (1). There is a lack of studies that have investigated potential pharmacological agents for the treatment of SOD. At present, studies have employed only small numbers of patients, and the majority of investigations into SOD therapy were not discussed (5,6); further investigation is therefore required.

It was previously demonstrated that feeding rabbits high-cholesterol diets can induce hypercholesterolemia (HC) and result in SOD (7); at present, the HC rabbit is the only SOD model available for study. Paeoniflorin (PF) is the major active ingredient in herbaceous peonies and is a traditional Chinese medicine that has been reported to relieve muscle spasms in clinical practice (8). PF can relax the gastrointestinal smooth

muscle (9), and our previous study revealed that PF can relax rabbit SO muscle rings *in vitro* (10).

Free Ca^{2+} in the cytoplasm of smooth muscle cells acts as a second messenger during smooth muscle relaxation and contraction. It has been reported that Ca^{2+}-induced smooth muscle contractions originate from the intracellular sarcoplasmic reticulum and extracellular fluid (11,12). It has also been proposed that the entry of extracellular Ca^{2+} into cells across the cell membrane may act as an inducer of intracellular Ca^{2+} release (11,12). Low concentrations of Ca^{2+} promote smooth muscle relaxation, whereas high concentrations induce smooth muscle contraction (13). Our previous study suggested that high cholesterol can increase the intracellular calcium ion concentration in rabbit SO, and that PF can reduce the intracellular calcium ion concentration in HC rabbits with SO in a dose-dependent manner (3); however, the underlying mechanism requires further investigation.

Ca^{2+} in the extracellular fluid can enter cells via voltage dependent calcium channels (VDCCs) in the cell membrane. These channels can be divided into the following subtypes: L-, T- and N-type (14). The VDCCs on the cell membrane of smooth muscles are predominantly composed of L- and T-types. Compared with that of L-type calcium channels, the density of T-type calcium channels has been associated with cell growth (14). Only a small number of T-type calcium channels are expressed on the cell membrane of smooth muscles compared with L-type calcium channels under normal conditions (15). Therefore, the L-type calcium channel may serve a critical role in the relaxation and contraction of smooth muscles. When the cell membrane of smooth muscle is depolarized, Ca^{2+} enters the cells via L-type calcium channels and acts as a major inducer of smooth muscle contraction (16). Therefore, the aim of the present study was to determine the effects of PF on the L-type calcium channel in the SO cells of rabbits with HC.

Additionally, the present study investigated whether increases in the intracellular Ca^{2+} concentration in the SO under HC conditions may be induced via activation of L-type calcium channels. Furthermore, the present study hypothesized that PF may inhibit the activity of L-type calcium channels and the influx of extracellular Ca^{2+} ions, and may reduce the intracellular Ca^{2+} concentration to induce SO muscle relaxation.

Materials and methods

Animals and drugs. Purebred, New Zealand, big-eared rabbits (n=60; 3-4 months of age; 1.5-2.0 kg) were obtained from the Experimental Animal Center of Dalian Medical University (Dalian, China). The 40 rabbits (19 females and 21 males) were screened with a total cholesterol content <3.0 mmol/l, which is considered to be healthy (17). The animals were acclimated to laboratory conditions (22±2˚C with a 12 h light/dark cycle and a relative humidity of 40-60%). All animals were treated humanely according to the guidelines of the Institutional Animal Care and Use Committee of Dalian Medical University (18). The present study was approved by the Animal Ethics and Welfare Committee of Dalian Medical University [SCXK (Liao) 2008-0002] and was performed in strict accordance with the UK Animals (Scientific Procedures) Act 1986, and the associated guidelines, the EEC Directive of 1986 (86/609/EEC) and the NIH guide for the care and use of laboratory animals (NIH Publication no. 80-23; revised 1978) (19). PF (standard product) was purchased from Chengdu Must Bio-Technology Co., Ltd., (Chengdu, China). Nimodipine (10 μmol/l) was obtained from Shandong Xinhua Pharmaceutical Co., Ltd., (Zibo, China). The concentration of nimodipine used for inhibiting the current was 10 μmol/l, with the duration of 5 minutes at room temperature.

Establishment of the high cholesterol model. The New Zealand rabbits were randomly divided into two groups: A control (CON) group with 10 animals and a HC group with 30 animals. Animals had free access to water. In the CON group, the animals were administered 300 g standard rabbit feed daily; the HC group were provided with 300 g of standard feed daily with an additional 1 g of cholesterol (purity, ≥99.0%; cat. no. C8280-500; Beijing Solarbio Science & Technology Co., Ltd., Beijing, China) for 6 days and then no cholesterol for 1 day. The animals were fed under the aforementioned weekly feeding schedules for a total of 8 weeks. Prior to experimentation, 0.5 ml of blood was taken from rabbit ear veins and the serum cholesterol concentration was measured with a total cholesterol assay kit (cat. no. A111-1; Nanjing Jiancheng Bioengineering Institute, Nanjing, China) according to the manufacturer's instructions. In brief, blood samples were centrifuged at 210 x g at 4˚C for 10 min, and the concentration of cholesterol in the supernatant was determined by colorimetric assay. A total of 40 rabbits whose cholesterol levels were below 3 mol/l were selected as subjects. According to the criteria for HC (7), a total cholesterol content <3.0 mmol/l was considered normal, whereas a total cholesterol content >10 mmol/l was considered as HC. Rabbits with a total serum cholesterol content >3.0 mmol/l were excluded.

Extraction of rabbit SO cells. CON and HC rabbits were anesthetized. A median incision was made in the upper abdomen and the SO segment was isolated without the nipple. Following the removal of mucosal and connective tissues from the surface, the remaining SO segment was cut into small sections (1 mm^3) and placed in 0.1% collagenase II and 0.01% soybean trypsin inhibitor; digestion was conducted at 37˚C for ~4 h, with agitation every 30 min. The tissue sections reduced in size, cell edges were less visible and the solution formed a suspension until numerous fusiform smooth muscle cells were observed under an inverted phase contrast microscope (magnification, x10; Olympus Corporation, Tokyo, Japan). Subsequently, the solution was filtered with a 50 μm sieve and centrifuged at a speed of 34 x g at room temperature for 5 min. The pellet was collected and resuspended in 4 ml RPMI-1640 medium (Gibco; Thermo Fisher Scientific, Inc., Waltham, MA, USA). Finally, trypan blue staining was performed to determine whether cell viability was >90%. The duration of staining was 3 min at room temperature and the cell concentration was $5x10^5$ cells/ml (in PBS). Cells were counted under a microscope (magnification, x10; Olympus Corporation, Tokyo, Japan) in three fields of view.

Cell identification. Cell morphology was determined using an inverted microscope (magnification, x400). The cells which were observed under an inverted microscope were cultured

in medium 199 (Gibco; Thermo Fisher Scientific, Inc.) with 10% fetal bovine serum (Gibco; Thermo Fisher Scientific, Inc.), 1% penicillin and streptomycin, as well as 5 ng/ml stem cell factor (SCF; PeproTech, Inc., Rocky Hill, NJ, USA) at 37˚C with 5% CO_2 for 48 h. Individual smooth muscle cells appeared fusiform or taeniform. The cytoplasm was abundant and dense; the cells were opaque. There were numerous cell protrusions and the nuclei were orbicular-ovate. At the center of cells, several plasmosomes were observed. As the cell density increased, the cells were arranged into parallel bundles, and some cells overlapped others, indicating growth. Cell density was at $5x10^5$/ml for further analysis.

Immunohistochemical detection. A total of $5x10^5$ cells/ml were added to a 60 mm culture dish containing a sterile coverslip (18x18 mm) coated with polylysine and placed in a 5% CO_2 incubator at a room temperature for 30 min. The cells were blocked in 5% bovine serum albumin (Hyclone; GE Healthcare Life Sciences, Logan, UT, USA) in a monolayer at a room temperature for 20 min, mouse anti-human α-smooth muscle actin monoclonal antibody (1:50; 50 μl; Santa Cruz Biotechnology, Inc., Dallas, TX, USA) was added and the cells were incubated at 4˚C for 8 to 12 h (until 80% confluence). Subsequently, a peroxidase-conjugated goat anti-mouse immunoglobulin G secondary antibody (cat. no. ZB-2305; 1:2,500; ZSGB-BIO, Inc., Beijing, China) at 37˚C for 20 min, followed by a horseradish peroxidase streptavidin conjugate reagent were added. The slides were then subject to staining with 3,3'-diaminobenzidine (Sigma-Aldrich; Merck KGaA, Darmstadt, Germany) for 5 min and mild hematoxylin (Nanjing Jiancheng Bioengineering Institute, Nanjing, China) counterstaining for 10 sec and examined under a microscope (x40; Olympus Corporation).

Preparation of in vitro muscle strip tissues and contraction experiments. New Zealand rabbits were anesthetized by an intraperitoneal injection of chloral hydrate, and the mucosal and connective tissues of the SO segment were removed as aforementioned. The SO segment was sectioned longitudinally to obtain 2x5 mm muscle strips. The ends of one muscle strip were ligated; one end was fixed to a glass hook at the bottom of the organ bath chamber, the other was connected to an RM6240C type tension transducer. The organ bath chamber was filled with Krebs solution and supplied with a mixture of 95% O_2 and 5% CO_2 at 37˚C. The tension transducer was connected to a multi-channel physiological signal amplifier. The detected signal was transmitted to a computer to record spontaneous contractions. An initial tension of 1.0 g was applied. After approximately 15-20 min, SO muscle strips appeared to have more regular amplitude of spontaneous stabilized contractions, and the value of the tension transducer reading was set to zero. The typical tension curves of spontaneous contractions of rabbit SO muscle were subsequently recorded in response to 0.1, 1.0 and 10.0 μmol/l PF. Contraction experiments were repeated three times.

Calcium fluorescence. Obtained SO cells ($5x10^5$/ml) were incubated in physiological saline solution (PSS) containing 1 μmol/l Fluo-3AM (cat. no. F8840; Beijing Solarbio Science & Technology, Co., Ltd.) and 0.02% F-127 for 1 h at 37˚C. Subsequently, the cells were placed in a perfusion chamber with a mixture of 95% O_2 and 5% CO_2. The intracellular Ca^{2+} concentration was determined by flow cytometry (excitation wavelength, 494 nm; emission wavelength, 516 nm).

Reverse transcription-quantitative polymerase chain reaction (RT-qPCR). SO cells of the HC group were divided into four subgroups and incubated in DMEM containing 0, 0.1, 1.0 or 10.0 μmol/l PF, respectively for 12 h. Total RNA was extracted using RNAiso Plus (Takara Biotechnology Co., Ltd., Dalian, China). cDNA was reverse transcribed and gDNA was removed with the PrimeScript RT Reagent Kit with gDNA Eraser (Takara Biotechnology Co., Ltd.), according to the manufacturer's protocol. The PCR experiments were performed with SYBRPremix Ex Taq (Takara Biotechnology Co., Ltd.) in an ABI 7500 Fast Real-Time PCR system (Qiagen China Co., Ltd., Shanghai, China). RT-qPCR was performed using the following primer sets: GAPDH sense, 5'-GGGTGG TGGACCTCATGGT-3' and antisense, 5'-CGGTGGTTTGAG GGCTCTTA-3'; α1C sense, 5'-CGCTATGGGCTATGAG CTA-3' and antisense, 5'-GAAAAAGGATCCAAAGA TGA-3'. The PCR thermocycling conditions were as follows: 40 cycles of denaturation at 94˚C for 30 sec, annealing at 53˚C for 30 sec and extension at 72˚C for 1 min. Final extension was performed at 72˚C for 5 min (20).

Whole cell patch-clamp preparation and experiments. The SO segment was digested as aforementioned and the cell suspension (1 ml) was added to the perfusion chamber. An inverted microscope was used to observe the cells at a low magnification (x100). The electrode tip was filled with the electrode solution [containing tetraethylammonium (TEA; 20 mmol/l), CsCl (110 mmol/l), EGTA 10, $MgCl_2$•$6H_2O$, HEPES, Na_2 adenosine 5'-triphosphate (ATP); all Sigma-Aldrich; Merck KGaA] by immersion and a syringe was used to apply additional electrode solution via the opposite end of the electrode. Following visualization under an inverted microscope, a glass electrode filled with intracellular solution was fixed in an electrode holder. The glass electrode was carefully positioned in the solution using a micromanipulator. The electrode tip was slowly transported closer to the cells using the micromanipulator and visualized using a high-magnification microscope (x40, Olympus Corporation, Tokyo, Japan). When the electrode was attached to a cell, the positive pressure (between -30 and -10 mV) was removed, and slight or no negative pressure was applied. Then, the cell membrane was tightly sealed by the electrode tip. The formation of a high resistance seal was indicated when the electrode resistance was >1 GΩ, for which the transmembrane current was recorded. Cells were continuously perfused by PSS solution containing Ba^{2+}. The cell membrane potential was analyzed at -80 mV and the time of depolarization was 400 msec. Current alterations were recorded during this time; the single depolarization pulse stimulation was increased from -80 mV and the stimulation was repeated every 10 sec. When the recorded current was stable, 0, 0.1, 1 μmol/l or 10 μmol/l PF was added to the extracellular solution of medium 199 (Gibco; Thermo Fisher Scientific, Inc.) with 10% fetal bovine serum (Gibco; Thermo Fisher Scientific, Inc.), 1% penicillin and streptomycin as well as 5 ng/ml SCF (PeproTech, Inc., Rocky Hill, NJ, USA) at

37˚C with 5% CO_2 for 48 h. The effects on the barium current (I_{Ba}) peak value were then determined. For these experiments, a PC-10 type microelectrode drawing instrument (Narishige Scientific Instrument Lab., Tokyo, Japan), an EPC-10 type patch clamp amplifier (HEKA Elektronik Dr. Schulze GmbH, Lambrecht, Germany) and a MP-225 type micromanipulator (Sutter Instrument, Novato, CA, USA) were used.

Statistical analysis. The experimental data were presented as the mean ± standard error of the mean of three repeats. Statistical analysis of the data was conducted using SPSS v.19.0 (IBM Corp., Armonk, NY, USA). One-way analysis of variance was performed, followed by further analysis with a Least Significant Difference post hoc test for multiple comparisons. P<0.05 was considered to indicate a statistically significant difference.

Results

Measurement of serum total cholesterol in rabbits. The serum levels of total cholesterol in rabbits in the CON and HC groups were presented in Table I. Prior to cholesterol feeding, no difference was detected between the two groups (n=10; P>0.05). Following feeding with a high cholesterol diet, the serum cholesterol concentrations of the HC group were significantly higher than those of the CON group (n=10; P<0.01).

Typical tension curves of spontaneous contractions of rabbit SO muscle in response to 0.1, 1.0 and 10.0 μmol/l PF are presented in Fig. 1. The spontaneous contractions of SO muscles in the CON and HC groups were analyzed (Fig. 1A). The statistical analysis of SO muscle responses were presented in Fig. 1B and Table II. The results indicated that treatment with various concentrations of PF reduced the tension of SO muscle strips in the CON and HC group. The tension observed with various concentrations of PF were significantly lower when compared with the HC group prior to PF administration.

Following 48 h of primary SO cell incubation with medium 119, adherent growth was observed. The cells appeared ribbon-shaped or spindle-shaped when viewed under an inverted microscope (Fig. 2A). Immunofluorescence staining of smooth muscle specific α-actin revealed a large number of filaments parallel to the long axis of the cells (Fig. 2B). The mean positive growth rate of the cells was >98% (data not shown).

Effects of PF on SO cell Ca^{2+} concentration. The effects of various concentrations of PF on alterations in the Ca^{2+} concentration of SO cells in the CON and HC groups are presented in Fig. 3A and Table III. The results indicated that 0.1 μmol/l PF did not notably affect Ca^{2+} concentrations in SO cells in the CON group; however, a significant decrease was observed in the HC group. Treatment with 1.0 and 10.0 μmol/l significantly reduced Ca^{2+} concentrations in the CON and HC groups when compared with no treatment (n=6; P<0.05; Fig. 3B).

L-type Ca^{2+} channel α1C subunit mRNA expression levels in response to PF. The results of RT-qPCR analysis demonstrated that the mRNA expression levels of the L-type Ca^{2+} channel α1C subunit were significantly higher in the SO cells of the HC group than in the SO cells of the CON group (n=8).

Table I. Serum levels of total cholesterol in rabbits (mmol/l).

Group	Prior to feeding	After feeding
Control	1.752±0.249	1.809±0.348[a]
Hypercholesterolemia	1.694±0.225	27.061±3.324[b]

Data are presented as the mean ± standard error of the mean. [a]P>0.05 vs. CON group prior to feeding. [b]P<0.01 vs. HC group prior to feeding.

Table II. Tension of sphincter of Oddi muscle strips with various concentrations of PF.

PF (μmol/l)	Control (g)	Hypercholesterolemia (g)
0.0	0.00	0.00
0.1	15.35±3.95	-40.32±11.31[a]
1.0	-29.75±4.27[a]	-180.20±12.92[b]
10.0	-33.75±4.15[a]	-210.70±14.47[b]

PF, Paeoniflorin. Data are presented as the mean ± standard error of the mean. [a]P<0.05, [b]P<0.01 vs. 0.0 μmol/l PF.

Table III. Alterations in Ca^{2+} concentration.

Paeoniflorin (μmol/l)	Control (%)	Hypercholesterolemia (%)
0.0	101.867±0.701	99.690±0.473
0.1	98.946±0.827	88.090±1.454[b]
1.0	93.370±1.643[a]	75.733±0.944[c]
10.0	84.363±0.601[a]	60.667±1.308[c]

Percentages represent the concentration of calcium ions. Data are presented as the mean ± standard error of the mean. [a]P<0.05 vs. control group treated with 0.0 μmol/l PF. [b]P<0.05, [c]P<0.01 vs. HC group treated with 0.0 μmol/l PF.

mRNA expression in SO cells treated with 0.1 μmol/l PF was not significantly different in the HC and CON groups (n=6); however, expression levels were significantly higher in the HC group than in the CON group (n=10) following treatment with 1.0 and 10.0 μmol/l PF (Fig. 4).

Effects of PF on the I_{Ba} peak values of SO cells from the CON group. When the membrane potential was clamped to -80 mV, step depolarization stimuli ranging from -60 to +60 mV elicited an inward current; this current was inhibited by nimodipine at 10 μmol/l for 5 min at room temperature, which suggested that the current was produced by the L-type calcium channel (I_{Ca}). As L-type Ca^{2+} channels are permeable to Ba^{2+}, this ion can be applied to measure the current conducted via the L-type Ca^{2+}channel (21). In addition, the properties of I_{Ba} and I_{Ca} are similar (21); as the amplitude of I_{Ba} recorded in this experiment was significantly larger than that of I_{Ca}, I_{Ba} was measured

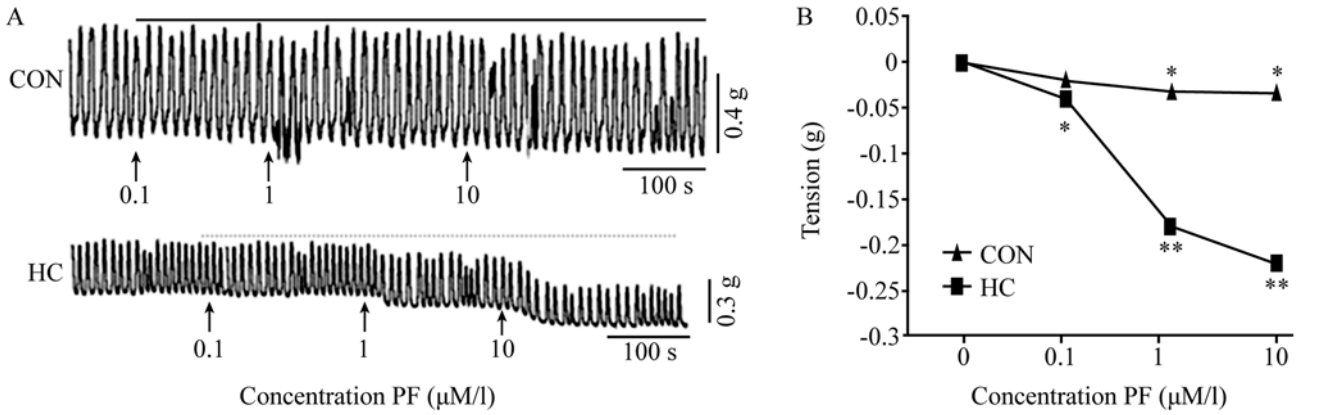

Figure 1. SO muscle contractions. (A) Spontaneous contraction of SO muscles in the CON and HC groups treated with different concentrations of PF. (B) Statistical analysis of SO muscle responses in the CON and HC groups with various concentrations of PF (as indicated). *P<0.05 and **P<0.01 vs. 0 μM/l PF. F/F0, fluorescence intensity ratio; CON, control; HC, hypercholesterolemia; PF, Paeoniflorin; SO, sphincter of Oddi.

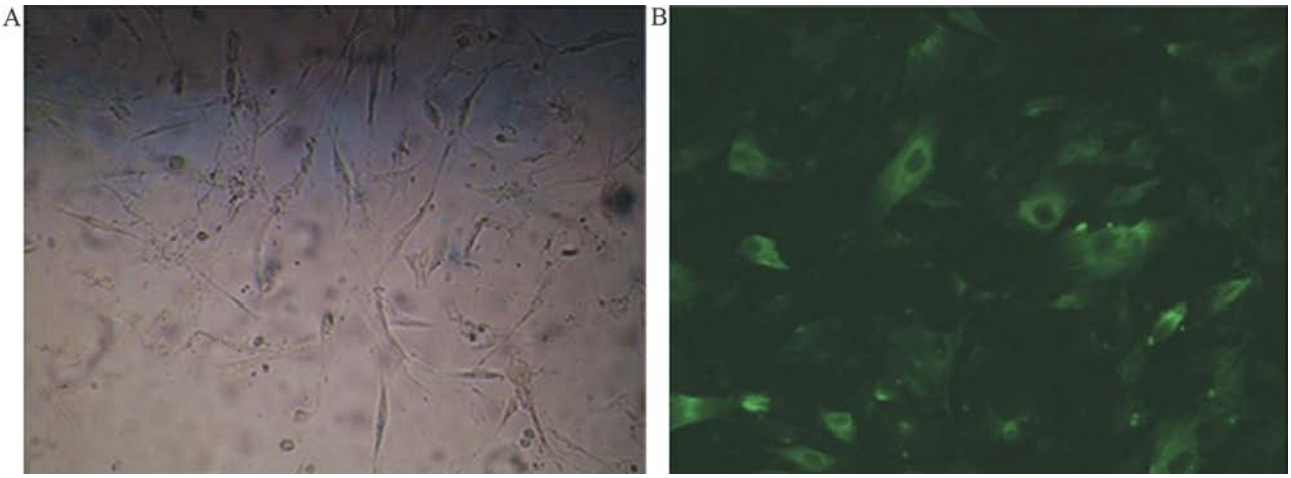

Figure 2. Morphology of sphincter of Oddi cells. (A) The cells appeared ribbon-shaped or spindle-shaped under an inverted microscope (x400). (B) Immunofluorescence staining of smooth muscle specific α-actin revealed an abundance of filaments parallel to the long axis of cells.

instead of I_{Ca} (data not shown). The results of the whole-cell patch-clamp recording method, and the current curve of the I_{Ba} prior to drug application and following the addition of 10.0 μmol/l PF to the CON group are presented in Fig. 5A. The results indicated that the peak I_{Ba} value in cells treated with 0.1 μmol/l PF was not significantly different from the value prior to drug application (n=8); however, the I_{Ba} peak values of cells treated with 1.0 and 10.0 μmol/l PF were significantly lower than that prior to drug application (n=6; Fig. 5B and C).

Effects of PF on I_{Ba} current-voltage (I-V) curves from the CON group. To detect the voltage dependence of the effect of PF on the I_{Ba} in SO cells from the CON group, the I-V curves prior to and following the addition of 10.0 μmol/l PF were plotted and alterations in I_{Ba} amplitude were analyzed. The results revealed that following the addition of 10.0 μmol/l PF to SO cells of the CON group, voltage pulses in the range of -20 to +40 mV I_{Ba} were markedly elicited when compared with that of SO cells without PF treatment (n=6; Fig. 5D and E).

Effects of PF on I_{Ba} peak values from the HC group. The results of the whole-cell patch-clamp recording method and the current curve of the I_{Ba} prior to drug application and following 10.0 μmol/l PF administration to the HC group are presented in Fig. 6A. The treatment of SO cells in the HC group with 0.1, 1.0 and 10.0 μmol/l PF significantly reduced the peak values of the I_{Ba} compared with that prior to drug application (n=8; Fig. 6B and C).

Effects of PF on the I_{Ba} I-V curve of SO cells from the HC group. To detect the voltage dependence of the effect of PF on the I_{Ba} in SO cells from the HC group, the I-V curves prior to and following the administration of 10.0 μmol/l PF were plotted and alterations in the I_{Ba} amplitude were analyzed. The results revealed that following treatment with 10.0 μmol/l PF, voltage pulses in the range of -20 to +40 mV I_{Ba} were markedly elicited compared with in SO cells of the HC group without treatment (n=6; Fig. 6D and E).

PF reduces I_{Ba} peak values. As presented in Fig. 7, treatment with 0.1 and 1.0 μmol/l PF reduced the I_{Ba} peak values markedly in the SO cells of the HC group when compared with that prior to drug application (n=6). Similarly, treatment with 10.0 μmol/l PF notably reduced the peak values of the CON group; however, a marked decrease was observed in the HC group when compared with prior to the application of PF (n=6; Fig. 7 and Table IV).

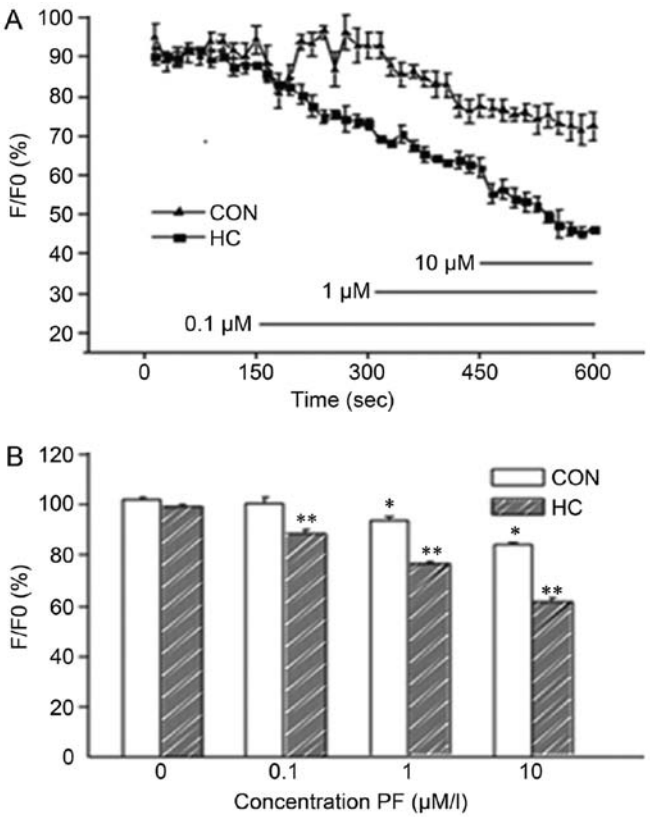

Figure 3. Ca^{2+} concentration in SO cells following PF treatment. (A and B) Effects and statistical analyses of different concentrations of PF on alterations in Ca^{2+} concentration in the SO cells of the CON and HC groups. *P<0.05 vs. 0 μM/l PF in the CON group; **P<0.01 vs. 0 μM/l PF in the HC group. F/F0, fluorescence intensity ratio; CON, control; HC, hypercholesterolemia; PF, Paeoniflorin; SO, sphincter of Oddi.

Table IV. Effects of PF on barium current peak values.

PF (μmol/l)	Control (%)	Hypercholesterolemia (%)
0.0	100.00±0.00	100.00±0.00
0.1	97.17±4.35	90.83±5.74[a]
1.0	86.85±3.26	83.32±4.92[a]
10.0	82.02±5.06	71.86±6.57[b]

PF, Paeoniflorin. Data are presented as the mean ± standard error of the mean. [a]P<0.05, [b]P<0.01 vs. 0.0 μmol/l PF.

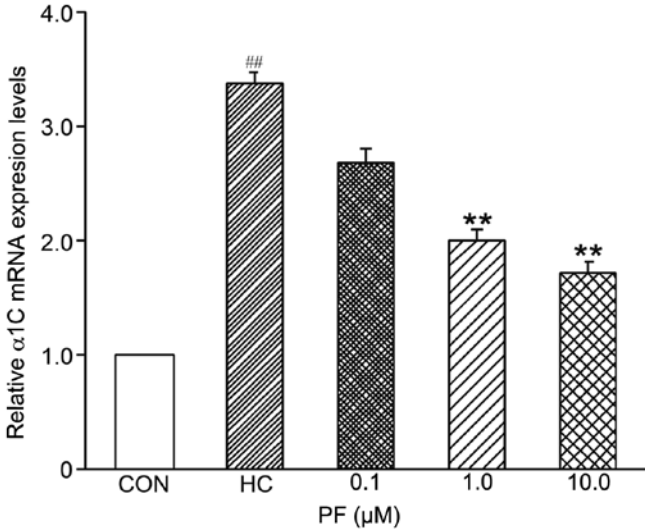

Figure 4. Reverse transcription-quantitative polymerase chain reaction analysis revealed that the mRNA expression levels of the α1C subunit of the L-type calcium channel in sphincter of Oddi cells in the HC group were significantly increased when compared with the CON group (n=8, $^{\#\#}$P<0.01). The 0.1 μM/l PF group had no significant differences when compared with the HC group (n=6; P>0.05). The 1 and 10 μM/l PF groups were significantly decreased when compared with the HC group (n=10; **P<0.01). CON, control; HC, hypercholesterolemia; PF, Paeoniflorin.

Discussion

A previous study demonstrated that disorders of cholesterol metabolism induce SOD. Szilvássy *et al* (22) reported a case of high cholesterol and hypertriglyceridemia associated with SOD, which suggested that patients with hyperlipidemia may also exhibit SOD. These observations may be due to hyperlipidemia, which leads to reductions in the levels of amyl nitrite in the body, inducing SOD. The results of Wei *et al* (7) revealed that feeding high cholesterol diets to rabbits induced HC. At present, the HC rabbit is the only model available to investigate SOD.

There is still no effective pharmaceutical treatment for SOD as a specific and long-acting drug with no adverse reactions. PF is the major active ingredient of herbaceous peonies, which are used in traditional Chinese medicine. Herbaceous peonies can be combined with other traditional Chinese medicines to produce traditional prescriptions, such as peony and licorice decoction. This particular prescription has been used in clinical practice to treat intestinal spastic abdominal pain and is notably effective (23). Recently, our group applied peony and licorice decoction in clinical practice to treat pancreatic and biliary SOD, with an ideal efficacy (24).

In addition, the effects of PF on the SO muscle ring of normal rabbits were observed and it was reported that PF significantly relaxed pre-constricted SO muscles (10); it was also revealed that PF relaxed SO muscle rings in HC rabbits (25). Additionally, laser confocal microscopy has demonstrated that high cholesterol can increase the intracellular Ca^{2+} concentration in rabbit SO. Conversely, PF can reduce intracellular Ca^{2+} concentrations in the SO of HC rabbits in a dose-dependent manner, which suggested that PF relaxes SO muscles via reductions in intracellular Ca^{2+} concentrations (3).

In the present study, the muscle strip tension experiment was conducted to observe the effects of PF on SO muscle strips from HC rabbits. The results demonstrated that the muscle strip tension of SO muscles from the CON and HC groups gradually decreased with increasing concentrations of PF. The effect was significant in the HC group when compared with the control. These observations were similar to those of our previous findings regarding the effects of PF on SO muscles rings in the CON and HC groups (3), indicating that PF can relax SO muscles.

A previous study using laser confocal microscopy revealed that Ca^{2+} concentrations increased in SO muscle cells within HC rabbits (3). This suggested that the increase in the Ca^{2+}

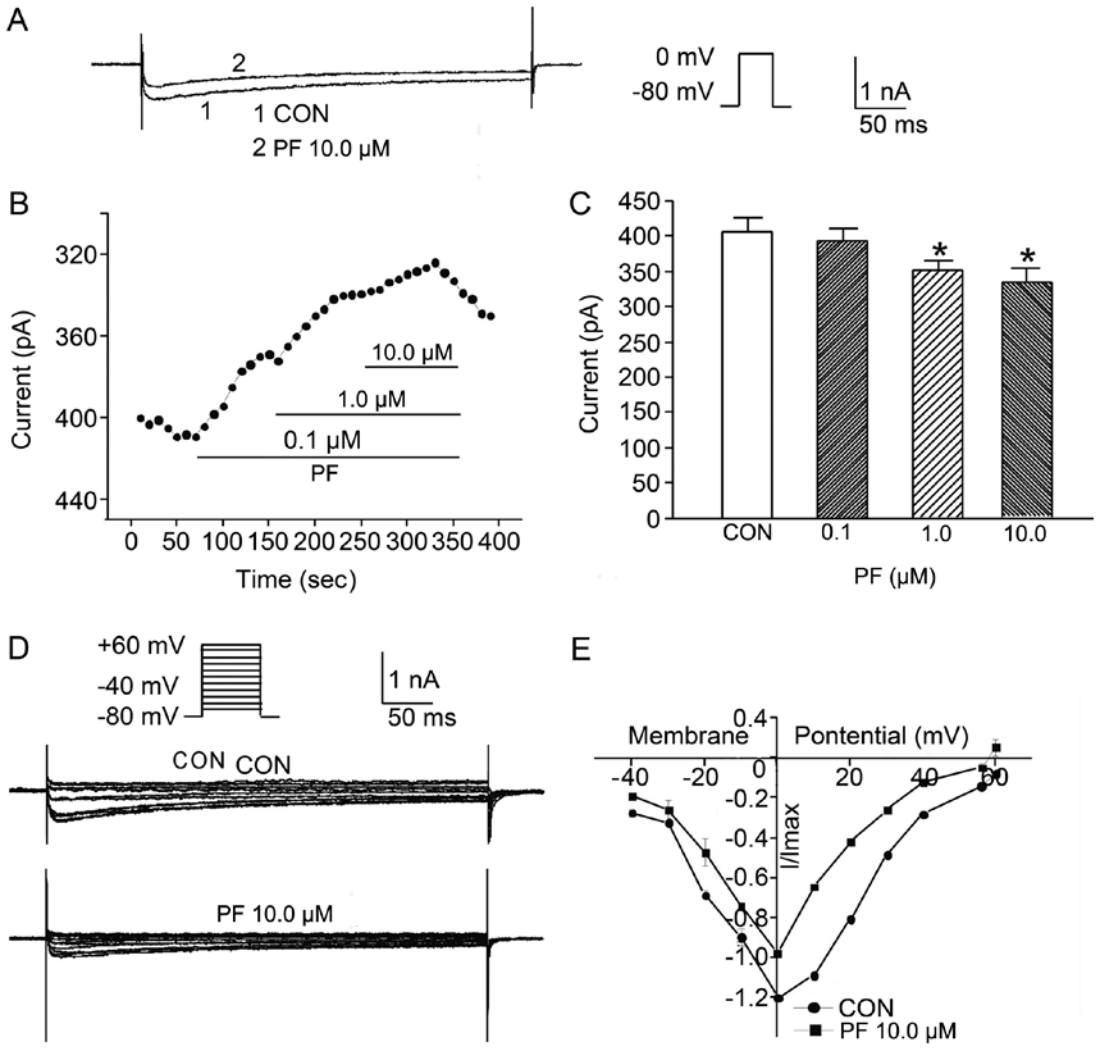

Figure 5. Effects of PF on I_{Ba} current-voltage curves from the CON group. (A) Current curve of the I_{Ba} prior to drug application and following the administration of 10.0 μmol/l PF to the CON group. The whole-cell patch-clamp recording method was applied as follows: Membrane potential was clamped at -80 mV and a single depolarization pulse stimulation was used directly from -80 to 0 mV at 10 sec intervals. (B and C) Various concentrations of PF (0.1, 1.0 and 10.0 μM) were added to the extracellular solution to observe the effects on the peak value of the I_{Ba}. The results indicated that the peak value of the I_{Ba} in response to 0.1 μmol/l PF was not significantly different from that observed prior to drug application (n=8), while the peak values of the I_{Ba} in response to 1.0 and 10.0 μmol/l PF treatment were significantly decreased when compared to that prior to drug application (n=6). (D and E) Effects of PF on the current-voltage curve of the I_{Ba} of the CON group. The results demonstrated that following the administration of 10.0 μmol/l PF to the extracellular solution, voltage pulses in the range of -20 to +40 mV I_{Ba} were markedly elicited (n=6). $^{*}P<0.05$ vs. CON. CON, control; I_{Ba}, barium current; PF, Paeoniflorin.

concentration may induce increased tension in SO muscles. In the present study, a different method was employed. Alterations in Ca^{2+} concentration were observed using calcium fluorescence, which demonstrated that PF may reduce the Ca^{2+} concentration in the SO muscle cells of normal and HC rabbits, and that this effect was concentration-dependent. Therefore, the relaxation of SO muscles induced by PF may be achieved via reductions in Ca^{2+} concentration.

The main sources of the Ca^{2+} that induce smooth muscle contraction are comprised of the intracellular sarcoplasmic reticulum and the extracellular fluid. It has been reported that the entry of extracellular Ca^{2+} into cells via the cell membrane induces the release of Ca^{2+} from the intracellular sarcoplasmic reticulum (13). A previous study indicated that L-type calcium channels serve a critical role in the relaxation and contraction of smooth muscle cells (16). During the depolarization of the smooth muscle cell membrane, Ca^{2+} enters cells via L-type calcium channels, which serves a major role in inducing smooth muscle cell contraction. The inhibition of L-type calcium channel activity may inhibit the transmembrane influx of extracellular Ca^{2+} and the release of intracellular Ca^{2+}, resulting in a reduction in the intracellular Ca^{2+} concentration (26).

The voltage-gated L-type calcium channel is a cell membrane protein complex. Upon depolarization of the membrane, the L-type calcium channel opens, permitting a large influx of Ca^{2+} into cells; the Ca^{2+} that enters the cells acts as a second messenger to regulate a variety of physiological processes, including muscle contraction, hormone secretion, neuronal transmission and gene expression (27). The physiological processes that depend on the activity of calcium channels to exert their functions include excitation-contraction, hormone secretion and transcription excitation coupling (11,12). The voltage-gated calcium channel

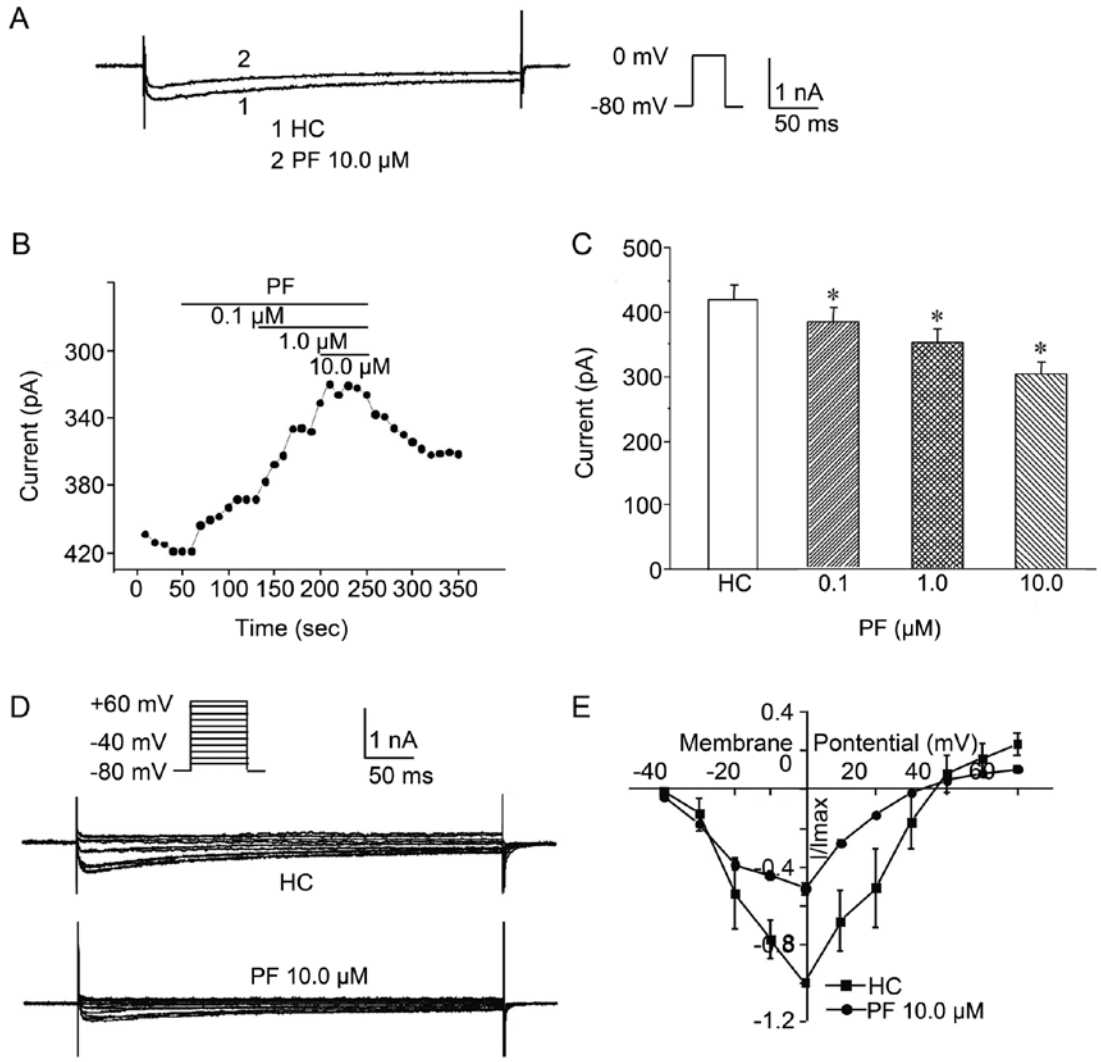

Figure 6. Effects of PF on I_{Ba} peak values from the HC group. (A) Current curve of the I_{Ba} prior to drug application and following the administration of 10.0 μmol/l PF to the sphincter of Oddi cells of the HC group. The membrane potential was clamped at -80 mV and a single stimulatory depolarization pulse was used directly from -80 to 0 mV at 10 sec intervals. (B and C) Treatment with 0.1, 1.0 and 10.0 μmol/l PF reduced the peak values of the I_{Ba} when compared with prior to drug application (n=8). $^*P<0.05$ vs. HC group. (D and E) Current-voltage curves prior to and following the addition of 10.0 μmol/l PF were plotted to analyze alterations in the I_{Ba} amplitude of cells prior to and following drug application. The results demonstrated that in response to 10.0 μmol/l PF added to the extracellular solution, voltage pulses in the range of -20 to +40 mV I_{Ba} were markedly elicited (n=6). HC, hypercholesterolemia; I_{Ba}, barium current; PF, Paeoniflorin.

is composed of at least four subunits; the α1 subunit consists of the selective pore for Ca^{2+}, as well as voltage sensors and binding sites of the main regulatory factors and drugs (11,12). The auxiliary subunits, α2δ, β and γ, are involved in transport, anchoring and regulation (28,29). Based on the α1 subunit, L-type calcium channels are classified as $Ca_v1.1$, $Ca_v1.2$, $Ca_v1.3$ or $Ca_v1.4$ (30). $Ca_v1.1$ expression has only been detected in skeletal muscles; however, some a previous study also observed human $Ca_v1.1$ co-expression with ryanodine receptors in γ-aminobutyric acid-ergic neurons (31). $Ca_v1.2$ is expressed in a variety of tissues, including the heart, smooth muscle, pancreas, adrenal gland and brain (32,33).

Additionally, $Ca_v1.3$ is mainly expressed in the brain and is expressed at lower levels than $Ca_v1.2$; expression has also been detected in the pancreas, kidneys, ovaries and cochlea (34). Furthermore, $Ca_v1.3$ has been detected in the sinoatrial node and is expressed in the atrium and cerebral ventricles in fetuses and newborn babies; however, low expression levels have also been reported in adult cerebral ventricles. At present, $Ca_v1.4$ expression has only been observed in the retina (34). The $Ca_v1.2$ channel is a protein complex composed of three subunits: α1, α2δ and β (35-37). The $Ca_v1.2$ calcium channel is abundant in a variety of animal tissues and serves important roles in the maintenance of central nervous system functions, the exertion of normal functions of the cardiac and smooth muscles, the regulation of the neuroendocrine system and other regulatory processes in the body (38).

In the present study, the effects of PF on voltage-gated L-type calcium channels in SO muscle cells were investigated in HC rabbits. The results of qPCR analysis revealed that the mRNA expression levels of the α1C subunit of the L-type calcium channel increased, suggesting that HC-induced SOD may be associated with the increased mRNA expression of this subunit. In addition, HC may cause an increase in L-type calcium channel activity. The mRNA expression levels of the α1C subunit of the L-type calcium channel decreased as

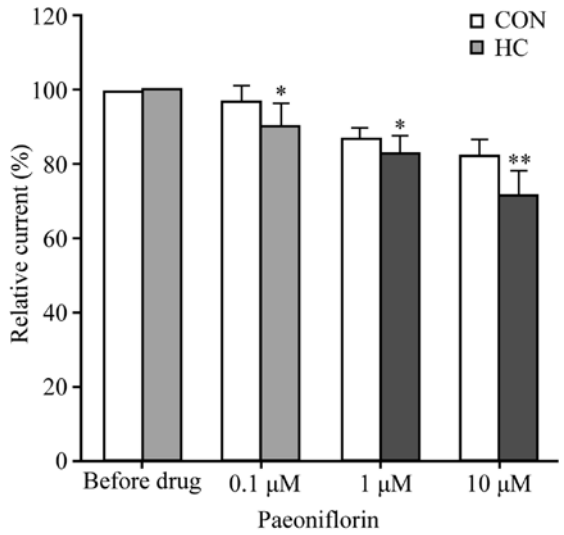

Figure 7. PF reduces I_{Ba} peak values. Treatment with 0.1 μmol/l PF reduced the peak values of the I_{Ba} of the SO cells in the CON and HC groups to 97.17±4.35 and 90.83±5.74% (n=6) prior to drug application, respectively; 1.0 μmol/l PF reduced the peak values in the CON and HC groups to 86.85±3.26 and 83.32±4.92% (n=6), respectively, when compared with prior to drug application, respectively. A total of 10.0 μmol/l PF reduced the peak values in the CON and HC groups to 82.02±5.06 and 71.86±6.57%, respectively (n=6) compared with prior to drug application. *P<0.05 and **P<0.01 vs. before drug application. CON, control; HC, hypercholesterolemia; I_{Ba}, barium current; PF, Paeoniflorin.

the concentrations of PF increased in the present study. This suggested that PF may reduce L-type calcium channel activity by decreasing Ca^{2+} influx and promoting the relaxation of SO muscle via reductions in the expression of the L-type calcium channel α1C subunit mRNA in SO cells.

The present study used whole-cell patch-clamping to record L-type calcium channel currents. The electrode solution contained TEA, CsCl, EGTA 10, $MgCl_2$•$6H_2O$, HEPES and Na_2 ATP; when the membrane potential was clamped to -80 mV, the application of depolarizing stimuli from -60 to +60 mV elicited an inward current. This current was inhibited upon the addition of nimodipine, suggesting that the current may be facilitated by the L-type calcium channel. Ba^{2+} served as the current carrier and I_{Ba} was investigated in the present study as the L-type calcium channel is highly permeable to Ba^{2+}, the properties of I_{Ba} and I_{Ca} are similar, and the amplitude of I_{Ba} is significantly larger than that of I_{Ca} (39), The results of the present study demonstrated that various concentrations of PF reduced the L-type calcium channel current in the SO cells of rabbits in the CON and HC groups; the effects of different concentrations of PF on the peak current values in the HC group were significantly lower than those in the CON group. In addition, PF reduced the expression of α1C subunits in SO cells from the CON and HC groups. Furthermore, PF effectively reduced L-type calcium channel activity, induced the relaxation of SO cells, inhibited the transmembrane influx of extracellular Ca^{2+} and reduced the number of smooth muscle cells induced by the L-type calcium channel, thereby inhibiting the release of intracellular Ca^{2+} and reducing the intracellular Ca^{2+} concentration.

In conclusion, the present study reported that PF induced the relaxation of SO muscle; possibly via a reduction in the Ca^{2+} concentration in the SO muscle cells of HC rabbits. PF also reduced the current of L-type calcium channels in the SO cells of HC rabbits in the present study. These results suggested that PF reduced intracellular Ca^{2+} concentrations via the reduction in L-type calcium channel activity and a decrease in the influx of extracellular Ca^{2+}. The resulting reduction in intracellular Ca^{2+} concentration may be the mechanism by which PF induces the relaxation of SO cells.

The results of the present study suggested that the underlying mechanism of PF on SO muscle relaxation may be associated with the reduction of Ca^{2+} influx via L-type calcium channels. These results provided theoretical support for the clinical treatment of SOD by using PF; however, other potential functions of PF on SO cells and the use of Chinese herbaceous peony as a therapeutic agent against SOD in association with SOD require further investigation.

Acknowledgements

Not applicable.

Funding

The present study was supported by the National Natural Science Foundation of China (grant no. 81774082).

Availability of data and materials

The datasets used and/or analyzed during the current study are available from the corresponding author on reasonable request.

Authors' contributions

FW, YY, CMW and YHW conceived and designed the study. YY established the high cholesterol model, and performed cell identification and the extraction of rabbit SO cells. FW prepared the *in vitro* muscle strip tissues and performed contraction experiments. XT performed the RT-qPCR. YY, FW and CMW performed the calcium fluorescence and whole cell patch-clamp preparation and experiments. XHJ and CMW performed data collection. FW, YY and XT performed the statistical analysis and preparation of figures. YHW performed the IHC experiments. YY, XT and YHW drafted the manuscript. All authors have read and approved the final manuscript.

Ethics approval and consent to participate

The present study was approved by the Animal Ethics and Welfare Committee of Dalian Medical University [Liaoning, China; SCXK (Liao) 2008-0002] and was performed in strict accordance with the UK Animals (Scientific Procedures) Act 1986, and the associated guidelines, the EEC Directive of 1986 (86/609/EEC) and the NIH guide for the care and use of laboratory animals (NIH Publication no. 80-23; revised 1978).

Patient consent for publication

Not applicable.

Competing interests

The authors declare that they have no competing interests.

References

1. Nakeeb A: Sphincter of Oddi dysfunction: How is it diagnosed? How is it classified? How do we treat it medically, endoscopically, and surgically? J Gastrointest Surg 17: 1557-1558, 2013.
2. Capodicasa E: Ruggero Oddi: 120 years after the description of the eponymous sphincter: A story to be remembered. J Gastroenterol Hepatolo 23: 1200-1203, 2008.
3. Wang F, Wang CM, Liu JD and Wang YT: Influence of paeoniflorin on intracellular calcium ion concentration in the sphincter of Oddi of hypercholesterolemic rabbits. Genet Mol Res 13: 5001-5010, 2014.
4. Vitton V, Ezzedine S, Gonzalez JM, Gasmi M, Grimaud JC and Barthet M: Medical treatment for sphincter of Oddi dysfunction: Can it replace endoscopic sphincterotomy? World J Gastroenterol 18: 1610-1615, 2012.
5. Rehman A, Affronti J and Rao S: Sphincter of Oddi dysfunction: An evidence-based review. Gastroenterol Hepatol 7: 713-722, 2013.
6. Li Y, He Y, Zhou Y and Chen X: Endoscopic sphincterotomy for sphincter of Oddi dysfunction. China Journal of Endoscopy 1: 108-110, 2002.
7. Wei JG, Wang YC, Du F and Yu HJ: Dynamic and ultrastructural study of sphincter of Oddi in early-stage cholelithiasis in rabbits with hypercholesterolemia. World J Gastroenterol 6: 102-106, 2000.
8. He W: Study on the mechanism of Peony and Licorice Decoction to relieving pain. J North Pharmacy 10: 101, 2013.
9. Yu WS, Ma T, Liu J and Qi QH: Research on the Effects and Ion Mechenism of paeoniflorin in regulating Gastrointestinal Motility. Basic Med Sci Clin 23: 111, 2003.
10. Luo JR, Wang CM, Fu L and Sun YP: Effects of paeoniflorin on contractile activity of rabbit sphincter of Oddi muscle rings in vitro. J Dalian Med Univ 31: 668-671, 2009.
11. Ma H, Groth RD, Wheeler DG, Barrett CF and Tsien RW: Excitation-transcription coupling in sympathetic neurons and the molecular mechanism of its initiation. Neurosci Res 70: 2-8, 2011.
12. Moosmang S, Kleppisch T, Wegener J, Welling A and Hofmann F: Analysis of calcium channels by conditional mutagenesis. Handb Exp Pharmacol 178, 469-490, 2007.
13. Hill-Eubanks DC, Werner ME, Heppner TJ and Nelson MT: Calcium signaling in smooth muscle. Cold Spring Harb Perspect Biol 3: a004549, 2011.
14. Jiang H and Stephens NL: Calcium and smooth muscle contraction. Mol Cell Biophys 135:1-9, 1994.
15. Dimopoulos GJ, Semba S, Kitazawa K, Eto M and Kitazawa T: Ca 2+ -dependent rapid Ca 2+ sensitization of contraction in arterial smooth muscle. Circ Res 100: 121-129, 2007.
16. Catterall WA: Voltage-gated calcium channels. Cold Spring Harb Perspect Biol 3: a003947, 2011.
17. Lasson A: The postcholecystectomy syndrome: Diagnostic and therapeutic strategy. Scand J Gastroenterol 22: 897-902, 1987.
18. Rowan AN: People for the Ethical Treatment of Animals v. Institutional Animal Care and Use Committee of the University of Oregon. Zoologica Africana 21: 89-94, 1986.
19. Hollands C: The Animals (Scientific Procedures) Act 1986. The Lancet 328: 32-33, 1986.
20. Livak KJ and Schmittgen TD: Analysis of relative gene expression data using real-time quantitative PCR and the 2(-Delta Delta C(T)) method. Methods 25: 402-408, 2001.
21. Hu ZY, Lin PT, Liu J and Liao DQ: Remifentanil induces l-type ca 2+, channel inhibition in human mesenteric arterial smooth muscle cells. Can J Anaesth 55: 238-244, 2008.
22. Szilvássy Z, Nagy I, Madácsy L, Hajnal F, Velösy B, Takács T and Lonovics J: Beneficial effect of lovastatin on sphincter of Oddi dyskinesia in hypercholesterolemia and hypertriglyceridemia. Am J Gastroenterol 92: 900-902, 1997.
23. Takao Y, Takaoka Y, Sugano A, Sato H, Motoyama Y, Ohta M, Nishimoto T and Mizobuchi S: Shakuyaku-kanzo-to (Shao-Yao-Gan-Cao-Tang) as treatment of painful muscle cramps in patients with lumbar spinal stenosis and its minimum effective dose. Kobe J Med Sci 61: E132-E137, 2016.
24. Song R, Wang CM, Xue WB and Ji XH: Preparation of serum containing drugs of Shaoyao Gancao Decoction and its effect on intracellular Ca2+ concentration of sphincter of Oddi in rabbits of hypercholesterolemic. Chinese Archives of Traditional Chinese Medicine 11: 2612-2615, 2014 (In Chinese).
25. Wang F, Luo JR and Wang CM: Effects of paeoniflorin on the sphincter of Oddi rings of hypercholesterolemia rabbits in vitro. China Health Care Nutrition 24: 456-457, 2014.
26. Quan X, Luo H, Liu Y, Xia H, Chen W and Tang Q: Hydrogen sulfide regulates the colonic motility by inhibiting both L-type calcium channels and BKCa channels in smooth muscle cells of rat colon. PLoS One 10: e0121331, 2015.
27. Pallone TL, Khurana S and Cao C: Voltage-Gated Calcium Channels: Structure and Function (CACNA) In Encyclopedia of Signaling Molecules. Choi S (ed). Springer, Cham, 2018.
28. Catterall WA: Structure and regulation of voltage-gated Ca2+ channels. Annu Rev Cell Dev Biol 16: 521-555, 2000.
29. Hofmann F, Biel M and Flockerzi V: Molecular basis for Ca2+ channel diversity. Annu Rev Neurosci 17: 399-418, 1994.
30. Ertel EA, Campbell KP, Harpold MM, Hofmann F, Mori Y, Perez-Reyes E, Schwartz A, Snutch TP, Tanabe T, Birnbaumer L, *et al*: Nomenclature of voltage-gated calcium channels. Neuron 25: 533-535, 2000.
31. Takahashi Y, Jeong SY, Ogata K, Goto J, Hashida H, Isahara K and Kanazawa I: Human skeletal muscle calcium channel alpha1S is expressed in the basal ganglia: Distinctive expression pattern among L-type Ca2+ channels. Neurosci Res 45: 129-137, 2003.
32. Moosmang S, Schulla V, Welling A, Feil R, Feil S, Wegener JW, Hofmann F and Klugbauer N: Dominant role of smooth muscle L-type calcium channel Cav1.2 for blood pressure regulation. EMBO J 22: 6027-6034, 2003.
33. Schulla V, Renström E, Feil R, Feil S, Franklin I, Gjinovci A, Jing XJ, Laux D, Lundquist I, Magnuson MA, *et al*: Impaired insulin secretion and glucose tolerance in beta cell-selective Ca(v)1. 2 Ca2+ channel null mice. EMBO J 22: 3844-3854, 2003.
34. Bock G, Gebhart M, Scharinger A, Jangsangthong W, Busquet P, Poggiani C, Sartori S, Mangoni ME, Sinnegger-Brauns MJ, Herzig S, *et al*: Functional Properties of a Newly Identified C-terminal Splice Variant, of Cav1.3 L-type Ca2+ Channels. J Biol Chem 286: 42736-42748, 2011.
35. Davies A, Hendrich J, Van Minh AT, Wratten J, Douglas L and Dolphin AC: Functional biology of the alpha(2)delta subunits of voltage-gated calcium channels. Trends Pharmacol Sci 28: 220-228, 2007.
36. Dolphin AC: Calcium channel auxiliary α2δ and β subunits: trafficking and one step beyond. Nat Rev Neurosci 13: 542-555, 2012.
37. Dolphin AC: Calcium channel diversity: multiple roles of calcium channel subunits. Curr Opin Neurobiol 19: 237-244, 2012.
38. Hofmann F, Flockerzi V, Kahl S and Wegener JW: L-type CaV1.2 calcium channels: From in vitro findings to in vivo function. Physiol Rev 94: 303-326, 2014.
39. Rosenberg RL, Hess P and Tsien RW: Cardiac calcium channels in planar lipid bilayers. L-type channels and calcium-permeable channels open at negative membrane potentials J Gen Physiol 92: 27-54, 1988.